PCCP

Accepted Manuscript

This is an *Accepted Manuscript*, which has been through the Royal Society of Chemistry peer review process and has been accepted for publication.

Accepted Manuscripts are published online shortly after acceptance, before technical editing, formatting and proof reading. Using this free service, authors can make their results available to the community, in citable form, before we publish the edited article. We will replace this *Accepted Manuscript* with the edited and formatted *Advance Article* as soon as it is available.

You can find more information about *Accepted Manuscripts* in the Information for Authors.

Please note that technical editing may introduce minor changes to the text and/or graphics, which may alter content. The journal's standard Terms & Conditions and the Ethical guidelines still apply. In no event shall the Royal Society of Chemistry be held responsible for any errors or omissions in this *Accepted Manuscript* or any consequences arising from the use of any information it contains.

ROYAL SOCIETY OF CHEMISTRY

www.rsc.org/pccp

Journal Name

ARTICLE TYPE

Cite this: DOI: 10.1039/xxxxxxxxxx

Correlation between diffusion barriers and alloying energy in binary alloys

Ulrik Grønbjerg Vej-Hansen,[ab] Jan Rossmeisl,[bc], Ifan E. L. Stephens,[a] and Jakob Schiøtz*[ab]

Received Date
Accepted Date

DOI: 10.1039/xxxxxxxxxx

www.rsc.org/journalname

In this paper, we explore the notion that a negative alloying energy may act as a descriptor for long term stability of Pt-alloys as cathode catalysts in low temperature fuel cells. Using density functional theory calculations, we show that there is a correlation between the alloying energy of an alloy, and the diffusion barriers of the minority component. Alloys with a negative alloying energy may show improved long term stability, despite the fact that there is typically a greater thermodynamic driving force towards dissolution of the solute metal over alloying. In addition to Pt, we find that this trend also appears to hold for alloys based on Al and Pd.

1 Introduction

Intermetallics with good resistance against diffusion have a number of important technological applications. An almost classical example is the use of Ni_3Al based "superalloys" in the aviation industry, for instance for turbine blades in jet engines, where the high diffusion barrier in the material, combined with ingenious design of the microstructure, reduce creep deformation [1]. Creep is the mechanism by which a material slowly changes shape under load, a problem that is strongly aggravated in jet engine turbines due to the high temperature combined with a very high mechanical tension due to centrifugal forces. A characteristic feature of these superalloys is that they have very negative alloying energies.

Similar design principles have been used for designing alloys in other harsh environments, one such example being the Oxygen Reduction Reaction (ORR) catalyst in low-temperature Polymer Electrolyte Membrane Fuel Cells (PEMFCs). For instance, alloys of Pt and late transition metals such as Ni, Cu, Co and Fe are often employed as cathode catalysts in Polymer Electrolyte Membrane Fuel cells. The catalysts are typically in nanoparticulate form, and need to withstand a very chemically aggressive environment with a high oxidation potential and low pH. This class of catalysts was first implemented in PEMFCs over two decades ago [2–5].

When commercial catalysts based on these alloys are implemented in fuel cells, they tend to degrade over time. The solute metal will tend to diffuse to the surface and dissolve into the electrolyte. This process is known as dealloying, and results in the catalytic activity decreasing towards that of pure Pt [6–9].

Such degradation limits the lifetime of PEMFCs with Pt alloys as cathode catalysts. Even so, there are numerous recent reports of novel forms of Pt-Ni based catalysts which show exceptionally high activity and stability, at least in accelerated degradation tests [10–13]. Nevertheless, it remains to be seen whether these catalysts will be able to maintain their superior performance over long periods of time [14].

In the search for new Pt-alloys for oxygen reduction, an earlier paper [15], co-authored by some of us, proposed that the alloying energy, or the enthalpy of formation, could also be used as a descriptor for stability for Pt alloys under PEMFC conditions. Some Pt rare earth alloys have exceptionally negative alloying energies, which could make them less susceptible to dealloying under PEMFC conditions. We discovered numerous ORR catalysts with negative alloying energies; in particular Pt_xY and Pt_xGd exhibit activity amongst the highest ever reported, both in the bulk polycrystalline and nanoparticulate form [15–19].

We note that although compounds such as Pt_3Y have a highly

[a] DNRF Center for Individual Nanoparticle Functionality (CINF), Department of Physics, Technical University of Denmark, DK-2800 Kgs. Lyngby, Denmark; E-mail: schiotz@fysik.dtu.dk
[b] Center for Atomic-scale Materials Design (CAMD), Department of Physics, Technical University of Denmark, DK-2800 Kgs. Lyngby, Denmark.
[c] Department of Chemistry, University of Copenhagen, DK-2100 København Ø, Denmark.

Physical Chemistry Chemical Physics Accepted Manuscript

negative alloying energy, they are thermodynamically more unstable than alloys such as Pt_3Ni under operating conditions. Indeed, the alloying energy tends to scale linearly with the dissolution potential of the transition metal [20]. However, while there are also results showing that the dissolution potential is perturbed by the interaction in an alloy, positive shifts were only observed for noble metals and they were much less common than negative shifts in the dissolution potential [21]. This leads us to ~~to~~ question whether it is the dissolution potential or the alloying energy that is more important in controlling the long term stability of Pt alloy catalysts in fuel cells.

In order to explore this notion experimentally, the catalysts would need to be tested over the long term in a PEMFC [14]. However, thus far, no synthesis method has been devised for alloys of Pt and rare earths that would yield a sufficient quantity of the catalyst for it to be tested in PEMFCs. The fact that similar compounds have already been produced leads us to take the view that this should eventually be possible [22–24].

On the contrary, in the current paper, we explore the notion with theoretical methods. We show that the alloying energy correlates strongly with the diffusion barrier of the alloying element. This implies that the high stability of the alloy would work as a kinetic barrier towards the dissolution of the highly reactive second component of the Pt alloy. We validate this assumption by showing that the diffusion barriers for vacancy diffusion scales with the alloying energy of the alloy.

2 Methods

We assume that solute metals transport from a Pt-alloy particle to the shell via diffusion. Interactions with adsorbed oxygen, either as a 2D adsorbate or as a 3D oxide phase, will only induce solute metal segregation between neighbouring atoms [25]. For example, it is unlikely that in a 3 nm particle adsorbed O or OH at the surface of the particle would interact directly with a solute metal atom in the core.

Usually, the dominant diffusion mechanism in metals is by vacancy diffusion along grain boundaries and dislocations, and there is no reason to believe that this is different in the alloys investigated in this work. In this work we investigate vacancy diffusion in defect-free, single-crystalline systems, as we take the view that any trend found here applies equally well to more realistic diffusion paths for larger systems. Furthermore, commercial Pt-based catalysts are often single crystalline [26], in which case bulk vacancy diffusion is likely to be the most relevant process.

Although most of the alloys under consideration have a relatively simple $L1_2$ crystal structure, modelling the diffusion process is computationally very demanding. For this reason, we only calculate the full diffusion path for a small number of alloys, and show that the diffusion barrier is well described by the energy of a characteristic configuration along the diffusion path, an energy that can be calculated with an order of magnitude lower computational cost. In these very stable alloys a significant energy is gained when the two different elements are next to each other, and conversely, a sizeable amount of energy is lost when this atomic arrangement is broken during the diffusion process.

We look at a vacancy diffusion path by exchanging the position of an atom of the ~~alloying~~ minority element with a vacancy. The simplest such diffusion path consists of six steps, involving a total of three atoms changing their lattice site. When all 6 steps have been completed, the crystal has regained its initial configuration, when translational symmetry is taken into account. The proposed diffusion path is shown in figure 1. It should be noted that the path is symmetric, with the 6 steps being pairwise mirror images of each other.

We have calculated the barrier for each step using the Nudged Elastic Band method [27–29], with the total barrier simply being the energy difference between the initial state and the transition state with the highest energy along the path. Two examples of the energies along the path are shown alongside the diffusion path in figure 1. We assume the vacancy concentration to be dominated by those created during synthesis or during the initial dissolution process on exposure to the electrolyte, and we assume that the variation in the diffusion rate is dominated by exponential dependence of the variation in the diffusion barrier rather than the vacancy concentration.

The interatomic interactions are described within the Density Functional Theory [30], using the PBE exchange-correlation functional [31]. The calculations were done using the GPAW DFT code [32] and the Atomic Simulation Environment (ASE) [33]. Due to the size of the calculations, the Kohn-Sham wavefunctions were described using a localized basis set within the Linear Combination of Atomic Orbitals (LCAO) formalism [34], using a Double-Zeta Polarised (dzp) basis set, from GPAW setups version 0.9.9672. The barriers were calculated in a 3 x 3 x 2 supercell, with the path being in the xy-plane. We used a 5 x 5 x 5 Monkhost-Pack grid [35] for sampling the k-space when doing calculations for the supercell used for calculating the barriers. The validity of the LCAO approximation was tested by calculating a few key energy differences using a full grid-based basis set, using a grid spacing of 0.18 Å. We calculated the total energy of the configurations A and B, as well as the one in the middle between them, in the LCAO geometry for Pt_3Y and Pt_3Cu, and found the shift in the total energy to be the same for the three configurations, within 140 meV for Pt_3Y and 14 meV for Pt_3Cu, indicating that the error in the barrier from using LCAO mode compared to FD, was on that order.

For all the alloys, we also calculated the alloying energy and the equilibrium lattice constant. The alloying energy is calculated with reference to bulk fcc Pt and the other metal in its most stable crystalline form. Here the number of k-points used depended on the element and its structural unit cell, but was never less than 6

Physical Chemistry Chemical Physics Accepted Manuscript

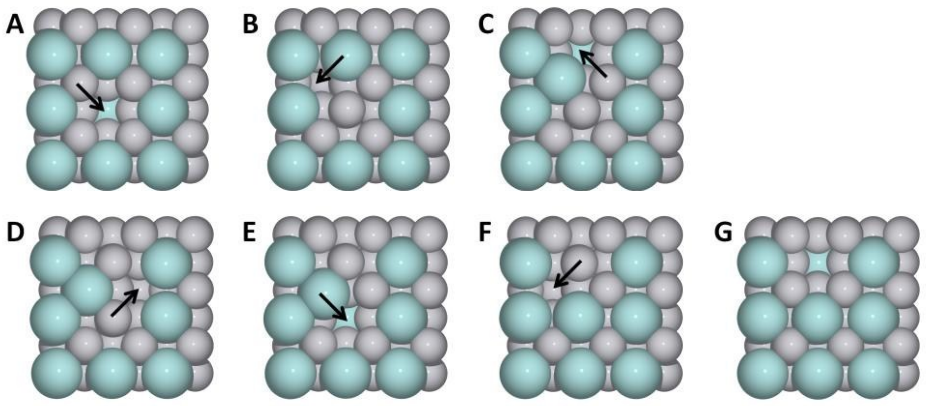

Fig. 1 The overall diffusion path. Here a top view of the computational unit cell is shown, which has a depth of two crystal unit cells. Here is shown Pt_3Y specifically, but it is equivalent for all alloys. To the right, the energy along the diffusion path is shown for both Pt_3Y in green and for Pt_3Cu in blue.

x 6 x 6, and usually at least 8 x 8 x 8, for a unit cell with at least 2 atoms. In all cases it was a result of a convergence test. Any calculation involving at least one of V, Cr, Mn, Fe, Co or Ni was spin-polarised. This resulted in a shift of as much as 350 meV per atom in the alloying energy compared to spin-paired calculations.

As the full diffusion path is demanding to calculate, we have calculated the barrier for a handful of alloys, chosen to be diverse with regard to alloying energy and lattice parameter. We expect that these two most important parameters are influencing diffusion: the alloying energy describes the strength of the interaction between the atoms, whereas the lattice parameter describes the space between the atoms along the diffusion path.

When atoms diffuse across surfaces, the lowest diffusion barriers often occur during the concerted motion of several atoms [36,37]. It is possible that something similar could occur here, i.e. that several of the fundamental steps in figure 1 occur simultaneously. To investigate this, we set up a large Nudged Elastic Band calculation with configuration A and D as the starting and ending point, and the three involved atoms moving simultaneously as the initial guess for the path. Since such a simulation is exceedingly demanding, we could only perform two calculations; we chose Pt_3Y and Pt_3Cu as two extreme cases, both with respect to alloying energy and size of the atoms. In both cases, the NEB calculations automatically split the motion into the three separate parts considered in this work, confirming that concerted motion of the atoms does not occur. Unlike at a surface, paths that involve motion of the atom out of the plane shown in Fig. 1 will either be symmetrically equivalent to the path investigated, or significantly more complicated.

Finally, we investigated the "direct" diffusion path, where the alloying atom moves directly from configuration A to G in figure 1 without a corresponding diffusive motion of the Pt atoms. For geometric reasons, we would only expect this to be possible for the smallest alloying atoms. Even in these cases, the barrier for direct diffusion is prohibitive. For example in Pt_3Cu, the direct diffusion barrier is 3.641 eV, whereas the barrier for the diffusion path in figure 1 is only 2.067 eV. Using a 3 x 3 x 3 supercell did not change this.

3 Results

We plot the barrier as a function of alloying energy and of the lattice parameter in figure 2. It is clearly seen that there is a significant correlation between the diffusion barrier and both the alloying energy and the lattice constant. As both the alloying energy and the size of the alloying atom and thus the lattice constant vary systematically through the periodic table, the two are clearly correlated, and it is *a priori* difficult to distinguish if the alloying energy or the lattice constant is the quantity that correlates most strongly with the diffusion barrier, and is thus the best predictor. In principle, this could be more rigorously investigated by performing the full diffusion barrier calculation on a large number of alloys: however, such an operation would be computationally too expensive. For this reason, on figure 3 we plot the energy difference, $E_{A\,!\,D}$, between the initial configuration and the middle of the diffusion path (labeled A and D in figure 1). There is a strong correlation, suggesting that $E_{A\,!\,D}$ is a major contributor to the diffusion barrier. The remainder of the diffusion barrier will then be the barrier between configurations C and D in figure 1. Furthermore, it turns out that the barrier height scales with the energy of the final state. This is commonly known as a Brønsted-Evans-Polanyi relation, and which is ubiquitous in chemistry [38,39] and has also been reported for surface diffusion of heteroelemental systems [40].

The strong correlation between $E_{A\,!\,D}$ and the barrier height allows us to estimate the barrier height on a much larger number of alloys, using around an order of magnitude less computational

Physical Chemistry Chemical Physics Accepted Manuscript

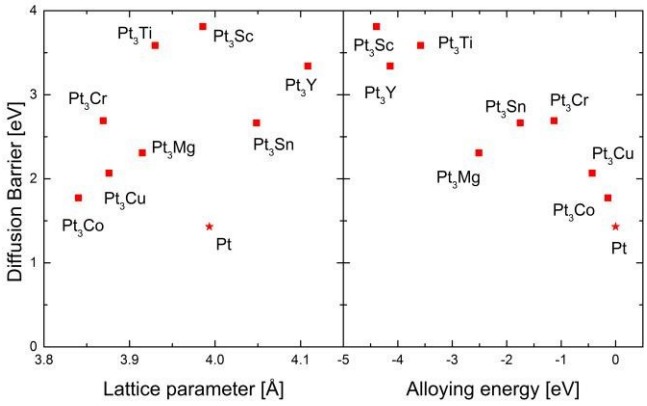

Fig. 2 Plot of the total barrier height vs. the lattice parameter of the alloy (left) and the alloying energy (right).

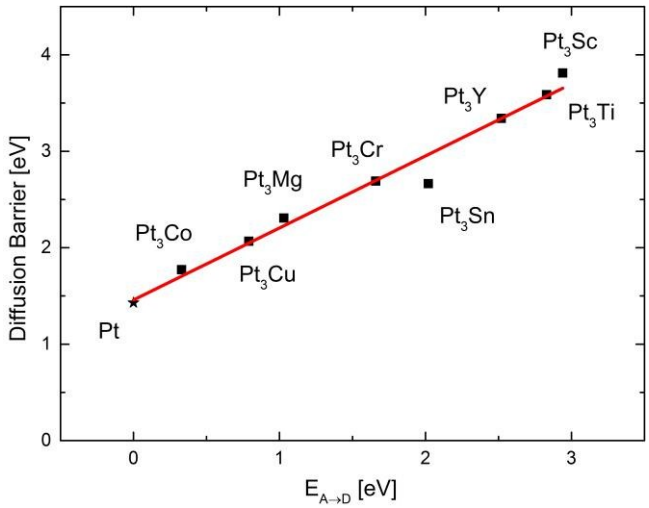

Fig. 3 The barrier height as a function of the energy difference between the initial and middle configurations on the diffusion path. These are shown as A and D in figure 1. The red line is a best linear fit with a slope of 0.75 ± 0.04 and an intercept of 1.46 ± 0.08 eV. It is seen that the correlation is very clear, indicating that this energy difference is a good descriptor for the barrier.

time than if we were to perform the full barrier height calculation on each of the alloys. The correlations between this energy difference and the alloying energy and the lattice constant are shown in figure 4(a) and 5, respectively.

Figure 4(a) shows that there is indeed a correlation between the alloying energy for the alloy and the specified energy difference. There is a significant amount of scatter, indicating that the alloying energy is not the only parameter determining the barrier height, as expected. Nevertheless, the alloying energy correlates with the diffusion barrier, making it a sensible predictor for the stability of the alloy. The barriers of self-diffusion are included in the figures as star-shaped points.

Figure 5 shows the relationship between $E_{A \to D}$ and the lattice parameter of the alloy; we see no clear correlation. This indicates that the diffusion barrier is not significantly determined by the size of the atoms and the space in the lattice.

To investigate if the trends observed here are specific to platinum alloys or represent a more general tendency, we extended the calculations to Pd_3X and Al_3X alloys, chosen because palladium is chemically very similar to platinum whereas aluminium is very different, and yet both form a significant number of 3:1 alloys. We selected alloys where the structure is either $L1_2$, or very similar to $L1_2$ (similar in the sense that the two kinds of atoms have the same first coordination shell as in the $L1_2$ structure, but in a different Bravais lattice, in much the same way that hcp and fcc are similar, both being closed-packed structures). In all cases, the calculations are done in the $L1_2$ structure. The results are shown in figure 4. We indeed see the same trends in these families of alloys. In the palladium alloys the trend is slightly less pronounced, whereas it is significantly stronger in the aluminium alloys with the exception of Al_3Ir and Al_3Pt, which for reasons unknown are complete outliers.

4 Discussion and experimental evidence

These calculations have been performed for one of the simplest possible crystal structures for ordered alloys. Nevertheless, we conjecture that the correlation between alloying energy and diffusion barrier is a general principle, also applicable to similar families of alloys with other crystal structures. This is analogous to the experimentally observed strong correlation between the barrier for autodiffusion of a pure metal and its melting point, where the ratio between the activation energy and the melting point is approximately the same for almost all simple metals [1].

Our results are consistent with the experimental work of Johansson *et al.*[41] and Schumacher *et al.*[42] They deposited metals on a single crystalline Pt substrate under ultra-high vacuum conditions, and investigated at which temperature the metal diffused away from the surface. Y on Pt(111) went subsurface at 800 K[41] while Cu went subsurface already at 460 K on Pt(111)[42]. In both cases the bulk crystal was pure Pt instead of an alloy as in our case, which could cause an additional geometric contribution to the barrier of Y compared to Cu. A similar experiment was carried out by Tang et al[43] for Ce on Pt(111), a system with an equivalent alloying energy as Y/Pt(111), where they found that Ce alloyed with Pt at 770 K.

We illustrate the overall dissolution process of a Pt_3X alloy in figure 6. In order to be dissolved, the alloying element must first reach the surface, that implies overcoming both the diffusion barrier in the bulk alloy itself, and in the Pt overlayer. Once the atom reaches the surface, it is oxidised in a complicated

Physical Chemistry Chemical Physics Accepted Manuscript

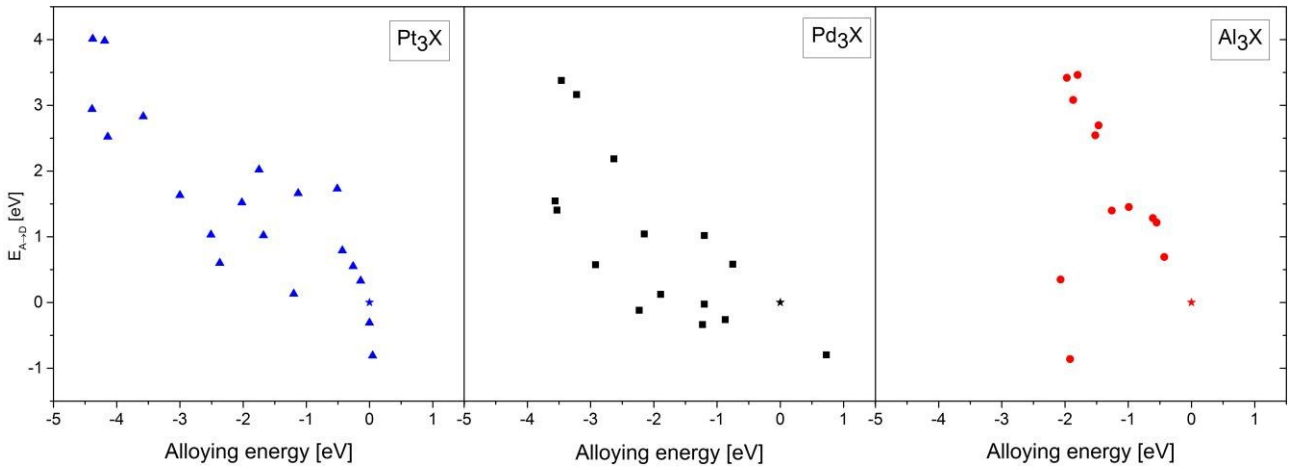

Fig. 4 The energy difference describing the diffusion barrier correlated with the alloying energy for Pd_3X (squares), Al_3X (circles) and Pt_3X (triangle) alloys. The autodiffusion for each main element is shown as a star and is by definition zero in this plot. In all three cases, we see a clear correlation. The outliers in the Al_3X set are Al_3Ir and Al_3Pt.

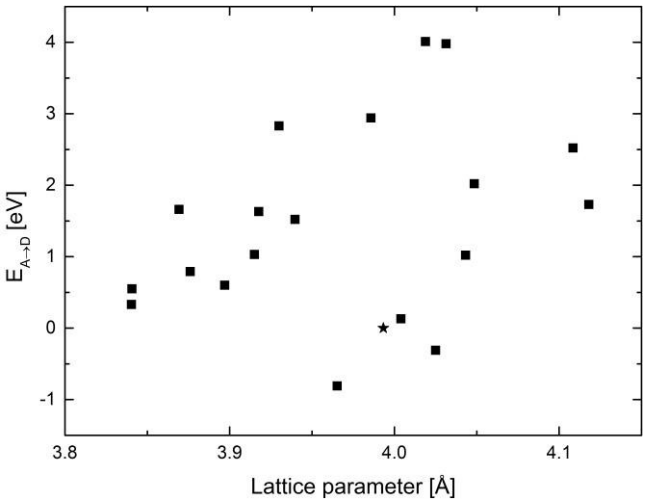

Fig. 5 The energy difference $E_{A\to D}$ vs. the lattice parameter of the alloy.

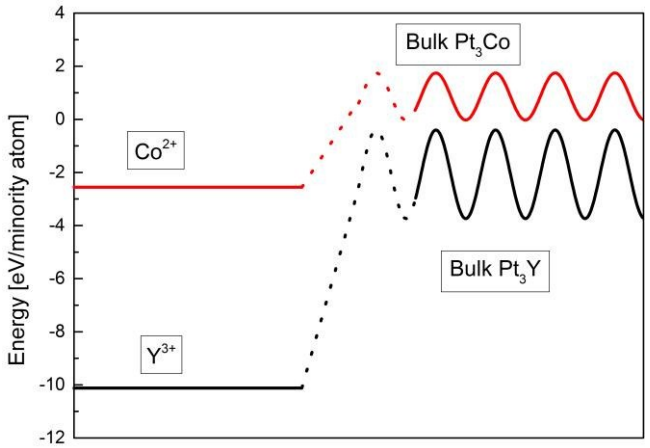

Fig. 6 Schematic overview of the energetics of the dealloying process in a PEM fuel cell with an electrode potential of 1 V vs. RHE. The focus of this work is the diffusion energy barrier in the metal. The energy barriers in the alloy, and the energy difference between the alloy and the dissolved atom are shown to scale. The energies of intermediate configurations relating to the dissolution process itself and passage through the near-surface region are unknown, as indicated by the dotted All other parameters are under

process, the details of which are beyond the scope of this paper. ~~Even so, we anticipate~~ It is clear that many processes may influence the dissolution process, including surface diffusion [45], oxide formation at the surface [46,47], details of the surface structure [21,48] and diffusion to the surface under influence of the adsorbed species [25]. If we assume that the barrier for diffusion in the bulk is comparable, if not greater than the barriers associated with the segregation of the solute metal to the surface and its subsequent dissolution [25]. ~~The~~, as supported by Menning and Chen [25], then the initial diffusion barrier provides the alloy with kinetic stability, in spite of the strong thermodynamic driving force toward oxidation. This barrier correlates with the alloying energy of the alloy; this causes the alloys of Pt and the early transition

Physical Chemistry Chemical Physics Accepted Manuscript

part of the lines. Everything else is standard conditions with the standard reduction potential from ~~ref~~the CRC Handbook of Chemistry and Physics.[44].

Physical Chemistry Chemical Physics Accepted Manuscript

metals to be ~~at~~ more stable toward diffusion-related degradation than the alloys with the late transition metals. This opens the possibility that they may display at least comparable stability under realistic operating conditions, in spite of the greater driving force for oxidation.

A further complication in fuel cell systems is the effect of the nanoparticulate form on the dissolution potential of the surface atoms. Several studies have shown how the dissolution potential is lower for Pt in the nanoparticulate form, an effect which can mainly be attributed to the surface curvature and the higher concentration of lower-coordinated atoms at corners, kinks and defects on the surface [21,49,50]. However, in systems of interest for the ORR, the surface will typically be comprised of Pt after exposure to reaction conditions [5], meaning this lowering of the dissolution potential should be approximately the same for all alloys.

Erlebacher and coworkers have suggested that surface diffusion plays an important role in dealloying [51] and in the formation of hollow nanoparticles from core-shell structures [45]. Surface diffusion leads to fluctuations of the outer surface, and a high probability of forming a pinhole in the shell, giving the electrolyte direct access to the non-noble core. In the case of Pt alloys, where the shell is formed by dealloying, we would expect the structure to be self-healing; if the electrolyte gains access to the core, a new protective layer is immediately formed by local dealloying. The fluctuations induced by surface diffusion will, however, undoubtedly be important for the formation of the shell structure, and may be governing for the growth of the thickness of the shell.

5 Conclusion

We have shown that the barrier for vacancy diffusion of the minority element in Pt_3X, Pd_3X and Al_3X alloys correlate with the alloying energy of the alloy. This validates the use of the alloying energy as a key parameter when searching for alloys that are stable against diffusion related degradation. A central example is the discovery of Pt_3Y and Pt_5Y alloys as electrocatalysts for the oxygen reduction reaction in fuel cells [15,16], where Pt_3Y was predicted to be active while having a large alloying energy, and subsequently shown in electrochemical experiments to be both active and stable. In this case a protective overlayer of pure Pt is formed at the surface of the alloy. A high alloying energy turns out to be more important than the thermodynamic driving force for oxidative corrosion of the minority element. This is because the diffusion of the alloying element to the surface is kinetically hindered by the large diffusion barrier.

Experimental alloying energies are known for many compounds, and can be calculated relatively easily and accurately for new materials [52]. Consequently, we confirm the notion that the alloying energy will be useful as a key search parameter when searching for new alloys for applications where the diffusive stability of the alloy is of importance.

Acknowledgements

For funding of this work we gratefully acknowledge The Danish National Research Foundation's Center for Individual Nanoparticle Functionality (DNRF54) .

References

1 M. F. Ashby and D. R. H. Jones, *Engineering Materials I: An introduction to Properties, Applications and Design*, Elsevier, 2005.

2 S. Mukerjee and S. Srinivasan, *J. Electroanal. Chem.*, 1993, **357**, 201–224.

3 S. Mukerjee, S. Srinivasan, M. Soriaga and J. Mcrreen, *J. Electrochem. Soc.*, 1995, **142**, 1409.

4 S. Mukerjee and J. McBreen, *J. Electroanal. Chem.*, 1998, **448**, 163–171.

5 T. Toda, H. Igarashi, H. Uchida and M. Watanabe, *J. Electrochem. Soc.*, 1999, **146**, 3750–3756.

6 S. Chen, H. A. Gasteiger, K. Hayakawa, T. Tada and Y. Shao-Horn, *J. Electrochem. Soc.*, 2010, **157**, A82.

7 K. J. J. Mayrhofer, K. Hartl, V. Juhart and M. Arenz, *J. Am. Chem. Soc.*, 2009, **131**, 16348–16349.

8 H. A. Gasteiger, S. S. Kocha, B. Sompalli and F. T. Wagner, *Appl. Catal. B Environ.*, 2005, **56**, 9–35.

9 H. L. Xin, J. A. Mundy, Z. Liu, R. Cabezas, R. Hovden, L. F. Kourkoutis, J. Zhang, N. P. Subramanian, R. Makharia, F. T. Wagner and D. A. Muller, *Nano Lett.*, 2012, **12**, 490–7.

10 C. Baldizzone, S. Mezzavilla, H. W. P. Carvalho, J. C. Meier, A. K. Schuppert, M. Heggen, C. Galeano, J.-D. Grunwaldt, F. Schüth and K. J. J. Mayrhofer, *Angew. Chem. Int. Ed. Engl.*, 2014, 14250–14254.

11 B. Han, C. E. Carlton, A. Kongkanand, R. S. Kukreja, B. R. Theobald, L. Gan, R. O'Malley, P. Strasser, F. T. Wagner and Y. Shao-Horn, *Energy Environ. Sci.*, 2015, **8**, 258–266.

12 C. Chen, Y. Kang, Z. Huo, Z. Zhu, W. Huang, H. L. Xin, J. D. Snyder, D. Li, J. A. Herron, M. Mavrikakis, M. Chi, K. L. More, Y. Li, N. M. Marković, G. A. Somorjai, P. Yang and V. R. Stamenkovic, *Science*, 2014, **343**, 1339–43.

13 X. Huang, Z. Zhao, L. Cao, Y. Chen, E. Zhu, Z. Lin, M. Li, A. Yan, A. Zettl, Y. M. Wang, X. Duan, T. Mueller and Y. Huang, *Science (80-.).*, 2015, **348**, 1230–1234.

14 L. Dubau, M. Lopez-Haro, L. Castanheira, J. Durst, M. Chatenet, P. Bayle-Guillemaud, L. Guétaz, N. Caqué, E. Rossinot and F. Maillard, *Appl. Catal. B Environ.*, 2013, **142-143**, 801–808.

15 J. Greeley, I. E. L. Stephens, A. S. Bondarenko, T. P. Johansson, H. A. Hansen, T. F. Jaramillo, J. Rossmeisl, I. Chork-

Physical Chemistry Chemical Physics Accepted Manuscript

endorff and J. K. Nørskov, *Nat. Chem.*, 2009, **1**, 552–556.
16 I. E. L. Stephens, A. S. Bondarenko, L. Bech and I. Chorkendorff, *ChemCatChem*, 2012, **4**, 341–349.
17 M. Escudero-Escribano, A. Verdaguer-Casadevall, P. Malacrida, U. Grønbjerg, B. P. Knudsen, A. K. Jepsen, J. Rossmeisl, I. E. L. Stephens and I. Chorkendorff, *J. Am. Chem. Soc.*, 2012, **134**, 16476–9.
18 P. Hernandez-Fernandez, F. Masini, D. N. McCarthy, C. E. Strebel, D. Friebel, D. Deiana, P. Malacrida, A. Nierhoff, A. Bodin, A. M. Wise, J. H. Nielsen, T. W. Hansen, A. Nilsson, I. E. L. Stephens and I. Chorkendorff, *Nat. Chem.*, 2014, **6**, 732–8.
19 A. Velázquez-Palenzuela, F. Masini, A. F. Pedersen, M. Escudero-Escribano, D. Deiana, P. Malacrida, T. W. Hansen, D. Friebel, A. Nilsson, I. E. L. Stephens and I. Chorkendorff, *J. Catal.*, 2015, **328**, 297–307.
20 B. Han, C. E. Carlton, J. Suntivich, Z. Xu and Y. Shao-Horn, *J. Phys. Chem. C*, 2015, **119**, 3971–3978.
21 J. Greeley, *Electrochim. Acta*, 2010, **55**, 5545–5550.
22 K. W. Lux and E. J. Cairns, *J. Electrochem. Soc.*, 2006, **153**, A1139.
23 D. Saha, E. D. Bojesen, K. M. O. Jensen, A.-C. Dippel and B. B. Iversen, *J. Phys. Chem. C*, 2015, 150515065226000.
24 C. Yan and M. J. Wagner, *Nano Lett.*, 2013, 1–4.
25 C. A. Menning and J. G. Chen, *Top. Catal.*, 2010, **53**, 338–347.
26 L. C. Gontard, L. Y. Chang, C. J. D. Hetherington, A. I. Kirkland, D. Ozkaya and R. E. Dunin-Borkowski, *Angew. Chemie - Int. Ed.*, 2007, **46**, 3683–3685.
27 H. Jónsson, G. Mills and K. W. Jacobsen, *K. W. Jacobsen*, 1998, pp. 385–404.
28 G. Henkelman, B. P. Uberuaga and H. Jónsson, *J. Chem. Phys.*, 2000, **113**, 9901.
29 G. Henkelman and H. Jónsson, *J. Chem. Phys.*, 2000, **113**, 9978.
30 W. Kohn and L. Sham, *Phys. Rev.*, 1965, **140**, 1133–1138.
31 J. Perdew, K. Burke and M. Ernzerhof, *Phys. Rev. Lett.*, 1996, **77**, 3865–3868.
32 J. J. Mortensen, L. Hansen and K. W. Jacobsen, *Phys. Rev. B*, 2005, **71**, 035109.
33 S. Bahn and K. W. Jacobsen, *Comput. Sci. Eng.*, 2002, 56–66.
34 A. H. Larsen, M. Vanin, J. J. Mortensen, K. S. Thygesen and K. W. Jacobsen, *Phys. Rev. B*, 2009, **80**, 195112.
35 H. Monkhorst and J. Pack, *Phys. Rev. B*, 1976, **13**, 5188–5192.
36 G. L. Kellogg and P. J. Feibelman, *Phys. Rev. Lett.*, 1990, **64**, 3143–3146.
37 C. Chen and T. T. Tsong, *Phys. Rev. Lett.*, 1990, **64**, 3147–3150.
38 J. N. Brønsted, *Chem. Rev.*, 1928, **5**, 231–338.
39 M. G. Evans and M. Polanyi, *Inertia and driving force of chemical reactions*, 1938.
40 H. Yildirim, S. K. Sankaranarayanan and J. P. Greeley, *J. Phys. Chem. C*, 2012, **116**, 22469–22475.
41 T. P. Johansson, E. T. Ulrikkeholm, P. Hernandez-Fernandez, M. Escudero-Escribano, P. Malacrida, I. E. L. Stephens and I. Chorkendorff, *Phys. Chem. Chem. Phys.*, 2014, **16**, 13718–25.
42 N. Schumacher, K. Andersson, L. C. Grabow, M. Mavrikakis, J. Nerlov and I. Chorkendorff, *Surf. Sci.*, 2008, **602**, 702–711.
43 J. Tang, J. Lawrence and J. Hemminger, *Phys. Rev. B*, 1993, **48**, 15342–15353.
44 P. Vanýsek, *Handbook of Chemistry and Physics - Electrochemical Series*, 2015.
45 J. Erlebacher and D. Margetis, *Phys. Rev. Lett.*, 2014, **112**, 155505.
46 D. Johnson, D. Napp and S. Bruckenstein, *Electrochim. Acta*, 1970, **15**, 1493.
47 M. Wakisaka, S. Asizawa, H. Uchida and M. Watanabe, *Phys. Chem. Chem. Phys.*, 2010, **12**, 4184.
48 C. D. Taylor, M. Neurock and J. R. Scully, *J. Electrochem. Soc.*, 2008, **155**, C407.
49 R. Jinnouchi, E. Toyoda, T. Hatanaka and Y. Morimoto, *J. Phys. Chem. C*, 2010, **114**, 17557–17568.
50 L. Tang, B. Han, K. Persson, C. Friesen, T. He, K. Sieradzki and G. Ceder, *J. Am. Chem. Soc.*, 2010, **132**, 596–600.
51 J. Erlebacher, M. J. Aziz, a. Karma, N. Dimitrov and K. Sieradzki, *Nature*, 2001, **410**, 450–453.
52 G. Jóhannesson, T. Bligaard, A. Ruban, H. L. Skriver, K. W. Jacobsen and J. K. Nørskov, *Phys. Rev. Lett.*, 2002, **88**, 255506.

Physical Chemistry Chemical Physics Accepted Manuscript